Insight into the Nonlinear Absorbance of Two Related Series of Two-Photon Absorbing Chromophores

Joy E. Rogers,*,†,‡ Jonathan E. Slagle,†,§ Daniel G. McLean,†,|| Richard L. Sutherland,†,|| Mark C. Brant,†,|| James Heinrichs,†,+ Rachel Jakubiak,† Ramamurthi Kannan,†,# Loon-Seng Tan,† and Paul A. Fleitz†

Materials and Manufacturing Directorate, Air Force Research Laboratory, Wright Patterson Air Force Base, Ohio 45433, UES, Inc., Dayton, Ohio 45432, AT&T Government Solutions, Dayton, Ohio 45324, Science Applications International Corporation, Dayton, Ohio 45431, Anteon Corporation, Dayton, Ohio 45431, and Systran Systems Corporation, Dayton, Ohio 45432

Received: January 3, 2007

A comprehensive photophysical study of the linear and nonlinear absorption properties has been carried out on two series of two-photon absorbing dyes to gain insight into how structure−property relationships influence observed nonlinear absorption. The materials studied consist of an electron accepting benzothiazole group connected to an electron donating diphenylamine via a fluorene bridging group. Two series differ from each other by the addition of one phenyl group and for each series one-arm (dipolar, AF240 and AF270), two-arm (quadrupolar, AF287 and AF295), and three-arm (octupolar, AF350 and AF380) versions were studied. Overall the AF240 series exhibits higher intrinsic two-photon absorption (TPA) cross-sections than the AF270 series as well as enhanced nanosecond nonlinear absorption, with an increase with number of branches. The enhanced nanosecond nonlinearity is understood by taking into account the contribution from the singlet and triplet excited states and was verified by a two-photon assisted excited-state absorption model that satisfactorily predicts the nonlinear absorption of the chromophores.

Introduction

The development of two-photon absorbing materials is a growing area of research, as evidenced by the numerous publications in the past fifteen years.[1,2] There are a host of uses for two photon absorbers that include use in optical data storage,[3] frequency upconverted lasing,[4] nonlinear photonics,[5] microfabrication,[6] fluorescence imaging,[7] and photodynamic therapy.[8] Two-photon absorbers provide an advantage in these applications because high-energy photophysical properties are activated by low energy near IR excitation resulting in greater material or tissue penetration than visible or UV light. Another advantage is that the quadratic dependence of the intensity on two photon absorption allows for more control and finer resolution in various applications such as microfabrication and fluorescence imaging.

Much effort at the Air Force Research Laboratory has gone into studying a series of two-photon absorbing chromophores identified as AFX.[2] The materials consist of some combination of an electron-donating group, an electron-accepting group, and a fluorene bridging group given the names AFX, where X is a number corresponding to a particular chromophore. These chromophores all contain a similar type geometry consisting of a D−π−A (donor group−π-conjugated group−acceptor group), A-π-A, or D-π-D geometry. Others have also synthesized similar fluorene containing molecules.[9] Within the AFX materials attempts were made to modify the chromophores by changing the conjugated bridge and increasing the length of pendent side chains, as well as increasing the π-donor and acceptor strength.[2b,i] It was found that the addition of moderately long alkyl pendants to the fluorene bridging group not only imparts additional solubility but also increases the measured effective two-photon cross-section. Improvements were also observed when changing the donor and acceptor groups. The series of chromophores have recently been expanded to include two- and three-arm chromophores that show improved two-photon absorption.[2d,g,j,k,l,p] An increase in the effective two photon absorption is observed in the three-arm or octupolar AFX chromophores, AF450, AF455, and AF457.[2l,n] In the literature this increase has been discussed as a cooperative enhancement of nanosecond two photon absorption in other types of multi-branched structures.[10] We recently concluded that the enhancement in the effective two photon absorption is a result of excited singlet−singlet and triplet−triplet absorption as the dominant source in the absorption in the nanosecond regime of several AFX molecules, and that the chief role of two-photon absorption is to populate these states.[11,12] Therefore, understanding both the one- and two-photon photophysical properties of a material is critical for insight into the nanosecond nonlinear absorption.

Here we take a systematic approach to understanding the structure−property effect of the addition of arms by synthesizing two sets of materials that contain a dipolar (one-arm), quadrupolar (two-arm), and octupolar (three-arm) chromophore. The structures of the two series of chromophores studied are shown in Figure 1. All molecules contain an electron donating diphenylamine/triphenylamine conjugated through a planar fluorene center and an electron withdrawing benzothiazole. The AF270 series only differs from the AF240 series by an additional phenyl group (triphenylamine) between the central fluorene and

* Corresponding author: E-mail: Joy.Rogers@wpafb.af.mil.
† Wright Patterson Air Force Base.
‡ UES, Inc.
§ AT&T Government Solutions.
|| Science Applications International Corporation.
+ Anteon Corporation.
# Systran Systems Corporation.

10.1021/jp070050r CCC: $37.00
Published on Web 02/22/2007

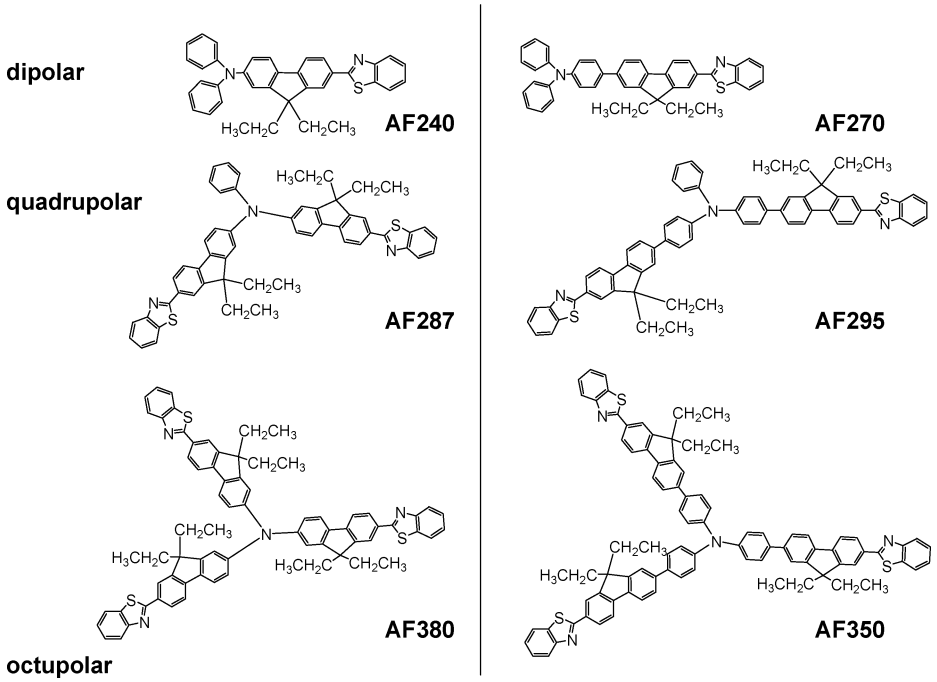

Figure 1. Shown are the structures of the AF240 series and the AF270 series. The dipolar molecules are AF240 and AF270. Quadrupolar are made up of two branches and are AF287 and AF295. AF380 and AF350 are octupolar containing three branches.

the nitrogen of the amine. These molecules have been discussed in some capacity separately in previous publications.[2d,e,g,i,k,l,m,o,p] Recently the one-photon ground-state absorption properties of these molecules were published in a report on theoretical molecular predictions,[2p] but to our knowledge a thorough structure property relationship study of these six chromophores has never been completed. In this paper we systematically compare the one-photon and two-photon photophysical properties within the series of chromophores to discern the structure property relationships based on a "dipolar versus quadrupolar versus octupolar" structural trend. We show that the kinetics and spectral properties obtained via one-photon excitation are needed to understand the significant differences of nonlinear absorption in the femtosecond and nanosecond domains.

Experimental

Synthesis. The synthesis of all materials has previously been described.[2p]

General Techniques. Ground-state UV/vis absorption spectra were measured on a Cary 500 spectrophotometer in a 1 cm path length quartz cuvette. Emission spectra were measured using a Perkin-Elmer model LS 50B fluorometer. Fluorescence measurements utilized a 1 cm path length four sided quartz cuvette. Phosphorescence measurements were done at 77 K in 2-methyltetrahydrofuran (MeTHF) using round quartz cells supplied by Perkin-Elmer. Approximately 20% MeI was added to each sample to enhance the formation of the triplet excited-state via an external heavy-atom effect. Phosphorescence data was collected at a delay time of 1 ms following the lamp pulse to eliminate fluorescence. Time-correlated single-photon counting (Edinburgh Instruments OB 920 Spectrometer) was utilized to determine singlet state lifetimes. The sample was pumped using a 70 ps laser diode at 401 nm. Emission was detected on a cooled microchannel plate PMT. Data was analyzed using a reconvolution software package provided by Edinburgh Instruments. Ultrafast pump−probe transient absorption measurements were performed using a 1-mJ, 100 fs pulse at 400 nm at a 1 kHz repetition rate obtained from a diode-pumped, Ti:sapphire regenerative amplifier (Spectra Physics Hurricane). The 800 nm beam was split and sent through a frequency doubler to create 400 nm light. The split beam was delayed and then focused into a sapphire plate to generate a white light continuum. The white light was then overlapped with the 400 nm pump beam in a 2-mm quartz cuvette and then coupled into a CCD detector. Details of the ultrafast system are described elsewhere.[2n] Nanosecond transient absorption measurements were carried out using the third harmonic (355-nm) of a Q-switched Nd:YAG laser (Quantel Brilliant, pulse width ca. 5 ns). Pulse fluences of up to 8 mJ cm^{-2} at the excitation wavelength were typically used. A detailed description of the laser flash photolysis apparatus has been published earlier.[13]

Fluorescence quantum yields were determined using the actinometry method previously described.[13] Quinine sulfate was used as an actinometer with a known fluorescence quantum yield of 0.55 in 1.0 N H_2SO_4.[14] All samples were excited at 350 nm with a matched optical density of 0.1. The molar absorption coefficient of the chromophore singlet excited-state was determined using the method of relative actinometry utilizing C_{60} in toluene.[15] The samples had matched optical density (OD) at the exciting wavelength of 400 nm. The molar absorption coefficient of the triplet excited-state was determined using the method of singlet depletion, which has been described previously.[13] Quantum yields for intersystem crossing were determined using the method of relative actinometry with a benzophenone actinometer.[13] Matched optical densities of the AFX molecule and benzophenone at 355 nm were utilized in each determination.

The two-photon absorption cross-sections were measured using the open aperture z-scan technique[16] with the concentrations of the samples in THF at 0.02 M unless otherwise noted. For these experiments we used a Spectra-Physics Hurricane Ti:Sapphire laser operating at 800 nm with a repetition rate of 1 kHz and pulse duration of 105 fs. Both the temporal and spatial profiles of the laser beam were Gaussian. In the Z-scan technique, a thin sample, meaning the path length through the sample is much less than the Rayleigh range of the optical path,

translates in and out of the focus of a laser beam and the transmission of the laser through the sample is recorded as a function of position along the optical axis (*z*-axis) with respect to the focal point. Z-scans were collected at various laser energies for each sample and the transmission profiles were fit to determine the two-photon absorption coefficient (β) and from that the two-photon absorption cross-section (σ_2). This procedure is described later in the manuscript. For our system the ($1/e^2$) radius of the beam at the focus (w_0) was 120 μm, giving a Rayleigh range of approximately 6 mm. On-axis intensity was measured with a Si photodiode and the laser beam profile was monitored with a WinCAD CCD array and software package from DataRay. Careful measurement of the on-axis laser intensity is necessary to get an absolute value for the two-photon absorption coefficient. To mitigate the effects of laser intensity fluctuations the laser beam is split into two arms, one for the sample (D_s) and the other for the reference (D_r) and the recorded transmission is the quotient of the two detectors (D_s/D_r).

Nanoscecond nonlinear transmittance measurements were performed with an optical parametric oscillator tuned to 800 nm. The pulse was Gaussian shaped with $\tau_L = 3.2$ ns. The beam was focused with an $f = 50$ cm lens into the sample. Over the length of the sample (1 mm) the beam was collimated. The beam shape was slightly elliptical, with a geometric-mean $1/e^2$ radius $w \approx 18.4 - 18.9$ μm, assuming an approximately Gaussian beam shape. The energy was varied, and incident and transmitted energies were measured with energy meters. To rule out the effects of self-focusing-defocusing we placed a large-area ($\sim$1 cm^2) detector near the exit of the sample to collect all transmitted energy. We also looked for stimulated backscattering by rotating the sample slightly to avoid Fresnel reflected light and measuring 180°-scattered light with an energy meter. At an incident pulse energy of 124 μJ, we measured $\sim$2 nJ of backscattered light. This would correspond to $< 2 \times 10^{-5}$ efficiency for stimulated scattering, which can be considered negligible compared with the nonlinear absorption loss.

Results

Ground-State Absorbance. Figure 1 shows the molecular structures of the chromophores designated as AF240, AF287, AF380, AF270, AF295, and AF350. Structurally all of these materials are similar except for the number of arms attached. Each arm consists of a D$-\pi-$A motif. A single arm is identified as dipolar, two arms are quadrupolar, and three arms are octupolar.[17] Between the AF240 and AF270 series the only difference is the presence of an extra phenyl ring between the fluorene and the nitrogen. To gain insight on the effect of altering the structure, ground-state absorption spectra (bold line) were measured in THF and are shown in Figure 2. The absorption intensity of each material has been quantified and is broad and structureless. A slight red-shift in the peak maximum is observed for both the AF240 and AF270 series with increasing branches (Table 1). A recent theoretical study of these two series of materials revealed that the strong absorption centered at 400 nm is due to an intramolecular charge transfer (ICT) absorption from the triphenylamine to the benzothiazole.[2p] Recently a thorough review on the formation of ICT states was published that details various mechanisms leading to the formation of this species.[18] In these materials the red shift is attributed to stabilization of the LUMO. An interesting thing to note is the blue shift in the peak of the AF270 series relative to the AF240 series. This blue shift is due to less formation of the ICT state in the AF270 series than in the AF240 series because of a longer π-conjugated region between the donor and acceptor.

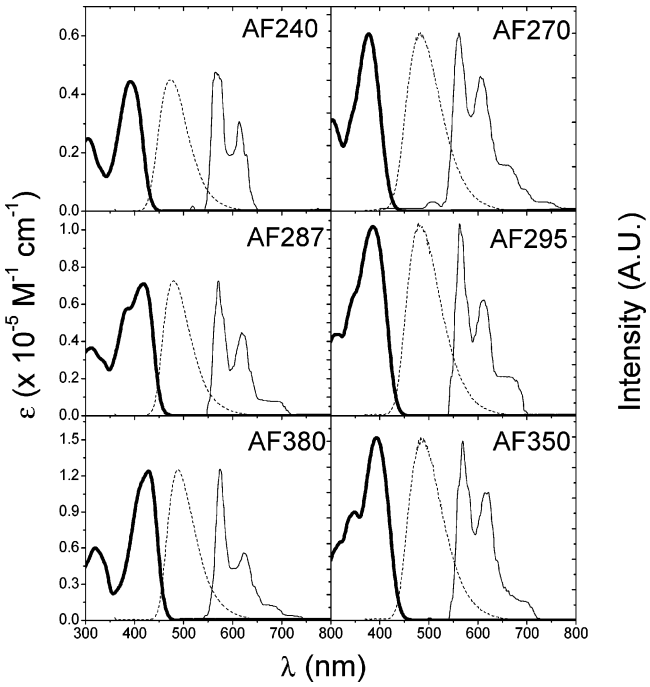

Figure 2. Absorbance (bold), fluorescence (dotted), and phosphorescence (solid) spectra of AF240, AF287, AF380, AF270, AF295, and AF350 in air-saturated THF. Fluorescence spectra obtained exciting at 350 nm at room temperature. Phosphorescence measurements were done at 77K in MeTHF exciting at the absorbance peak of each material. Absorbance values are in measured units on the left axis while fluorescence and phosphorescence are in arbitrary units on the right.

Steady-State Emission. Also shown in Figure 2 is the fluorescence spectrum (dashed line) of each chromophore in air saturated THF. Through a series there is only a minimal red-shift with increasing conjugation. However, a significant Stokes shift in the fluorescence is observed for all six chromophores (Table 1). Fluorescence excitation spectra were also measured (Supporting Information) and found to overlay very well with the ground-state absorbance data indicating that there is only one absorbing species present. The origin of this red shift is due to emission from a lower energy−solvent stabilized ICT (intramolecular charge transfer) state.[19] Upon vertical excitation to the localized excited-state a great deal of vibrational relaxation and solvent reorganization results in a stabilized lower energy state and a large red shift. To further confirm that the red shift is that of an ICT state, a brief solvent study was done for AF240 in hexane, benzene, THF, and acetonitrile and is shown in the Supporting Information. For AF240 we observe dual fluorescence from both the LE (localized excited state) and the ICT state in benzene.[18] Polar aprotic solvents, such as THF and acetonitrile, stabilize the ICT state through increased Van der Waals interactions of the solvent and solute and thus produce larger Stokes shifts.[18,19] The fluorescence quantum yields obtained in air saturated THF are given in Table 1. The trend observed is that the quantum yield decreases slightly from dipolar to octupolar in both series.

Phosphorescence data for each chromophore was obtained at 77 K in 2-methyltetrahydrofuran (MeTHF), and the data are shown in Figure 2 (solid line). Approximately 20% MeI was added to each sample to enhance the formation of the triplet excited state via an external heavy-atom effect. As with the fluorescence data, there is only a slight red-shift in the emission with increased branches for the two series. We determined the triplet excited-state energy from the blue edge of the phospho-

TABLE 1: Summary of Photophysical Properties in THF

	AF240	AF287	AF380	AF270	AF295	AF350
Abs_{max}	392 nm	418 nm	429 nm	377 nm	386 nm	393 nm
ϵ (M^{-1} cm^{-1})	44400 ± 2200	70900 ± 1300	123700 ± 900	60700 ± 1600	101700 ± 2800	152100 ± 2700
Fl_{max}	473 nm	481 nm	489 nm	483 nm	483 nm	486 nm
Φ_{fl} air saturated	0.649	0.609	0.516	0.765	0.701	0.594
Stokes shift	0.54 eV	0.39 eV	0.35 eV	0.72 eV	0.64 eV	0.61 eV
Ph_{max}	569 nm	571 nm	575 nm	561 nm	563 nm	569 nm
E_T	2.23 eV	2.22 eV	2.19 eV	2.26 eV	2.25 eV	2.23 eV
$S_1-S_{n\,max}$	623 nm	608 nm	618 nm	725 nm	595 nm	610 nm
ϵ (M^{-1} cm^{-1})	78800 ± 3900	54600 ± 4000	60100 ± 2000	70500 ± 3500	50200 ± 2500	62500 ± 3100
$T_1-T_{n\,max}$[a]	760 nm	810 nm	890 nm	520 nm	520 nm	530 nm
ϵ (M^{-1} cm^{-1})[a]	25100 ± 1300	47900 ± 2400	53000 ± 2700	48300 ± 2400	56700 ± 2800	81200 ± 4100
Φ_{ISC}air saturated	0.064 ± 0.007	0.074 ± 0.004	0.130 ± 0.039	0.031 ± 0.005	0.050 ± 0.002	0.035 ± 0.003

[a] Deoxygenated by three freeze pump thaw cycles

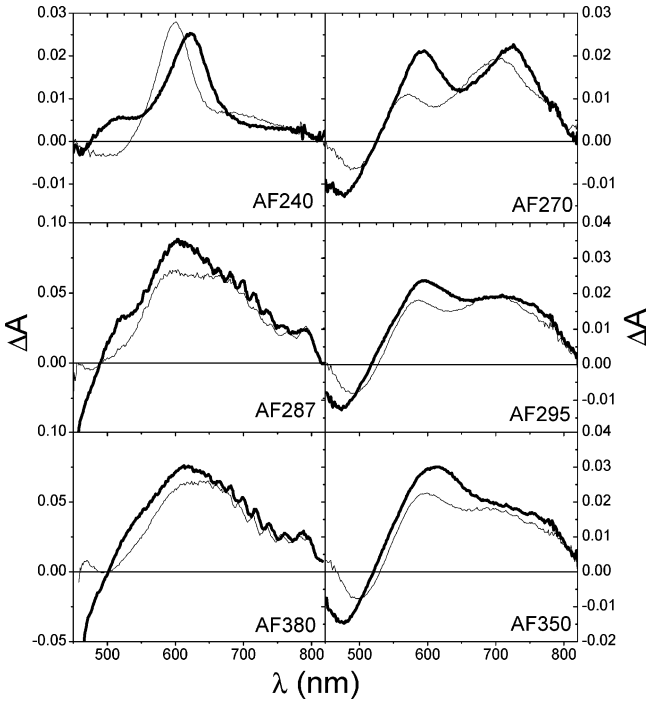

Figure 3. Shown above are the S_1-S_n spectra of AF240 (117 μM), AF287 (74 μM), AF380 (61 μM), AF270 (138 μM), AF295 (55 μM), and AF350 (34 μM) in air-saturated THF. Two times are shown, ~ 0 ps (bold) obtained immediately following the 100 fs 400 nm pulse and 10 ps (solid) after the laser pulse.

rescence spectra. This data is given in Table 1 along with the phosphorescence maximum.

Time-Resolved Excited State Properties. Time-resolved absorption was utilized to gain insight on both the decay kinetics and the spectral properties of the chromophores. Shown in Figure 3 are transient absorption spectra of all chromophores in air saturated THF immediately following 100 fs excitation at 400 nm (bold) and 10 ps (solid) after the pulse. In each of the chromophores we observe a transient at approximately time zero that shifts to form a new species in less than 3 ps. The specific lifetime for this change is given in Table 2 as τ_1. This change is attributed to formation of the ICT state and solvent reorganization for increased stabilization of the ICT state. Immediately after Franck−Condon excitation, only the electronic polarization of the solvent has adjusted to the new enlarged dipole so the solvent reorients into a lower energy equilibrated state.[20] The trend observed is that with increasing branches to the chromophore the lifetime is longer. Therefore, in the larger octupolar materials, it takes more time for the solvent to reorganize around the chromophore to stabilize the charge transfer. Steric hindrances in the octupolar and quadrupolar species that are not as prevalent in the dipolar chromophores may be the cause of the increased lifetime. It takes a longer time for the solvent to reorient and equilibrate around the bulkier groups into the correct dipole with the ICT state. For the AFX transient at approximately time zero, we were able to quantify the spectra using C_{60} in toluene as an actinometer.[15] These results are given in Table 1. For both series we found that the molar absorption coefficient of the singlet excited-state at the peak for the dipolar species is largest then followed by the octupolar and finally the quadrupolar.

In addition to measuring the steady-state fluorescence, we also looked at the time-resolved fluorescence using time correlated single photon counting exciting at 400 nm. The lifetimes obtained are given in Table 2 as τ_2. The lifetimes in air saturated THF show no trend with structure differences. They are all around 2 ns.

Nanosecond laser flash photolysis was utilized to obtain the T_1-T_n excited-state spectra of each chromophore in deoxygenated THF. Upon 355 nm excitation the spectra obtained are shown in Figure 4. Unfortunately, due to a small intersystem crossing quantum yield (Table 1) the transient spectra are noisy. We were able to quantify the spectra using the method of singlet depletion. For the AF240 series we observed a red shift in the transient species along with an increase in the overall molar absorption coefficient. This follows the trend observed for the ground-state absorbance spectra indicating an increase in the overall conjugation in the quadrupolar and octupolar chromophores. In the AF270 series, the peak maximum is shifted to the blue relative to the AF240 series. With increasing branches a slight red shift in the T_1-T_n spectra is observed as well as an increase in the molar absorption coefficient. Of the two series, the AF270 series has the larger triplet molar absorption coefficient due to increased conjugation through the additional phenyl ring.

All materials in deoxygenated THF were found to decay biexponentially upon 355 nm excitation. The respective lifetimes are given in Table 2 as τ_3 and τ_4. A shorter decay with a lifetime around 100 μs was observed followed by a long-lived transient ranging from 500 μs to 1 ms. Comparing the spectral details at time zero overlaid with the longer lived transient (data not shown) there is a difference in the spectra indicating a new transient is being formed. Based on our previous study of AF455 it is possible that the new transient is due to an ICT state formed via the triplet excited state.[2n] The triplet excited-state lifetime measured in air saturated THF is also given in Table 2.

Femtosecond Two Photon Absorption. In an open aperture z-scan measurement, the change in transmission of the laser beam is measured as the sample translates toward and away

TABLE 2: Excited State Kinetics of AF240 and AF270 Series in THF

	τ_1 (air saturated)	τ_2 (air saturated)	τ_3 (air saturated)	τ_3 (deoxygenated)	τ_4 (deoxygenated)
AF240	0.93 ps	2.03 ns	227 ns	97 μs	~1 ms
AF287	1.92 ps	1.88 ns	211 ns	135 μs	503 μs
AF380	2.53 ps	1.85 ns	112 ns	87 μs	943 μs
AF270	1.35 ps	1.89 ns	444 ns	123 μs	539 μs
AF295	1.98 ps	1.88 ns	151 ns	140 μs	452 μs
AF350	2.71 ps	1.99 ns	152 ns	113 μs	438 μs

from the focus of the beam. The shape of the transmission profile follows eq 1 for a Gaussian temporal profile of the incident laser pulse:

$$T = \frac{1}{\sqrt{\pi} q_0} \int_{-\infty}^{+\infty} \ln[1 + q_0 \exp(-x^2)]\, dx \qquad (1)$$

where $q_0 = \beta I_0 L(1 + z^2/z_r^2)^{-1}$, L is the sample thickness (1 mm), I_0 is the on-axis laser intensity, z is the position on the optical axis with respect to the focus of the beam, and z_r is the Rayleigh length, typically 6 mm for our system. Raw data are given in the Supporting Information. Fitting of the transmission profiles to eq 1 yields values for the effective TPA coefficient, β_{eff}. This value is an "effective" TPA coefficient because it includes contributions from TPA and excited-state absorption, which derives from a three-level model that takes into account excited-state absorption following TPA.[21] Assuming that the excited-state absorption depends only on the population in the excited-state derived from a TPA process, as linear absorption at 800 nm is negligible, it is possible to describe the propagation equation in terms of TPA ($\sigma_{2\text{PA}}$) and excited state (σ_{ESA}) cross-sections, as shown by eq 2:

$$\frac{dI}{dz} = -\sigma_{2\text{PA}} N_0 I^2 - \sigma_{\text{ESA}} N_k I \qquad (2)$$

where I is the intensity of the laser as it propagates through the sample, N_0 is Avogadro's number, and N_k is the two-photon excited-state population

$$N_k \approx \frac{\sigma_{2\text{PA}} N_0 \tau_p I_0^2}{2h\nu} \sqrt{\frac{\pi}{2}} \qquad (3)$$

with the laser pulse width as τ_p, I_0 for the on-axis laser intensity and $h\nu$ the photon energy. Further evaluation of eq 2, including factoring out I^2 and taking a Taylor series expansion on the Gaussian pulse profile to the lowest order, leads to an expression for the effective TPA coefficient as a function of laser intensity as shown below in eq 4:

$$\beta_{\text{eff}}(I_0) = \beta\left(1 + \frac{\sigma_{\text{ESA}} \cdot \tau_p I_0}{2h\nu} \sqrt{\frac{\pi}{2}}\right) \qquad (4)$$

In Figure 5 these data are plotted for each dye studied and the two-photon absorption coefficient was determined by dividing the value for β by Avogadro's number (N_0) and the concentration of the sample (d) in mol/L:

$$\sigma_{2\text{PA}} = \beta / N_0 d \qquad (5)$$

The intrinsic TPA cross-section values are given in Table 3 for the AF240 and AF270 series of chromophores. A direct comparison of the two series indicates that the AF240 series had higher cross-sections than the AF270 series and that the cross-sections increased going from dipolar to octupolar architectures.

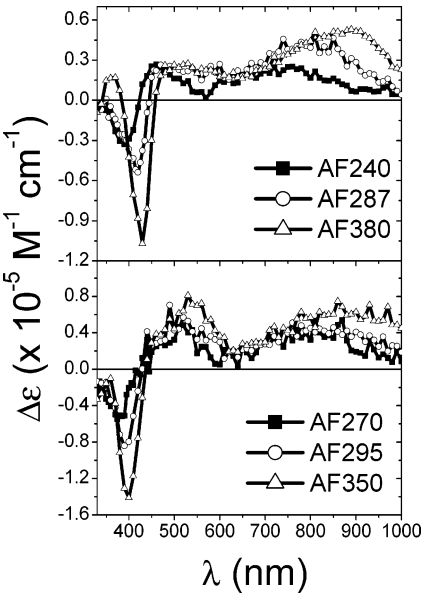

Figure 4. T_1-T_n absorption spectra observed after nanosecond pulsed 355 nm excitation of AF240 (25.9 μM), AF287 (7.3 μM), AF380 (11.2 μM), AF270 (4.8 μM), AF295 (4.1 μM), and AF350 (3.1 μM) in deoxygenated THF. Samples were deoxygenated by the freeze pump thaw method. Molar absorption coefficients were obtained by using the method of singlet depletion.

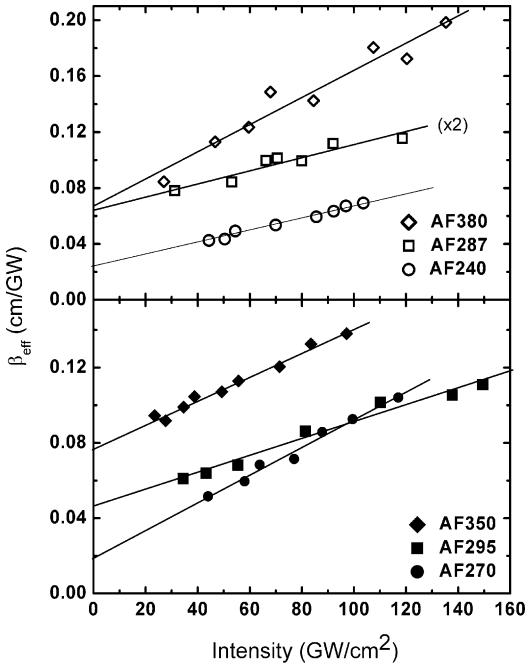

Figure 5. Plots of β_{eff} as a function of on-axis laser intensity for AFX dyes as indicated in the foreground of the panels. Lines through the points are fits to eq 4 in the text. y-intercepts are proportional to the intrinsic two-photon absorption cross-section (σ_2). For AF287 the data was multiplied by two because of the half concentration.

TABLE 3: Comparison of One Photon and Two Photon Properties in THF at 800 nm (unless Noted)

	fs TPA σ_2 (10^{-20} cm^4/GW)	S_1-S_n σ_s (cm^2)	T_1-T_n σ_T (cm^2)	Φ_T air saturated	sum $\Phi_T*\sigma_T$	ns TPA σ_2 (10^{-20} cm^4/ GW)
AF240	0.185 ± 0.015	1.45×10^{-17}	7.45×10^{-17}	0.064	0.48×10^{-17}	50 ± 8 39.3 ± 0.59[a]
AF287	0.495 ± 0.038	4.39×10^{-17}	15.9×10^{-17}	0.074	1.18×10^{-17}	99 ± 15
AF380	0.634 ± 0.016 0.39 ± 0.04[b]	6.08×10^{-17}	17.2×10^{-17}	0.130	2.24×10^{-17}	119 ± 18 92 ± 14[c]
AF270	0.146 ± 0.005 0.20 ± 0.02[b]	4.93×10^{-17}	15.3×10^{-17}	0.031	0.47×10^{-17}	29 ± 5
AF295	0.315 ± 0.014 0.31 ± 0.03[b]	5.80×10^{-17}	16.6×10^{-17}	0.050	0.83×10^{-17}	78 ± 12
AF350	0.489 ± 0.054 0.53 ± 0.05[b]	6.91×10^{-17}	22.0×10^{-17}	0.035	0.76×10^{-17}	139 ± 21 96 ± 14[c]

[a] Kannan, R. et al. *Chem. Mater*. **2001**, *13*, 1896. 800 nm; 8 ns pulse width. [b] He, G. S. et al. *J. Chem. Phys*. **2004**, *120*, 5275. 790 nm; 140 fs pulse width. [c] Kannan, R. et al. *Chem. Mater*. **2004**, *16*, 185. 800 nm; 8 ns pulse width.

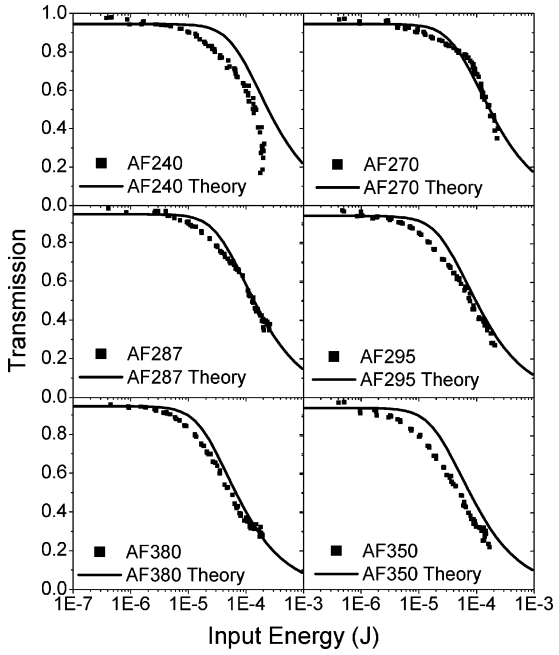

Figure 6. Nanosecond nonlinear transmission data for AF240 (0.0206 M), AF287 (0.0099 M), AF380 (0.0201 M), AF270 (0.0198 M), AF295 (0.0202 M), and AF350 (0.0195 M) in air-saturated THF as a function of laser pulse energy at 800 nm. Also shown is theoretical data calculated using an analytical effective three-photon absorption model based on the properties given in Table 3.

Nanosecond Nonlinear Transmission. Shown in Figure 6 are the nonlinear transmission plots for all six chromophores in air-saturated THF pumping at 800 nm with various energies. The samples were prepared to be around 0.02 M except for AF287, which was made to be 0.0099 M due to solubility limits. Measurements were made using a 1 mm quartz cuvette. Using the measured intrinsic σ_2 values and other measured photophysical parameters in Table 3, we calculated the NLT for each material and compared these calculations with the data shown in Figure 6. The calculation is based on an analytical effective three-photon absorption model of two-photon-induced excited-state absorption that was previously described in detail.[11] The energy transmittance for a sample of thickness L in this model is given by

$$T = \frac{T_0^2}{\sqrt{\pi} p_0} \int_{-\infty}^{+\infty \ln} \{[1 + p_0^2 \exp(-2x^2)]^{1/2} + p_0 \exp(-x^2)\}\, dx \quad (6)$$

where $p_0 = (2\gamma T_0^2 I_0^2 L)^{1/2}$, T_0 is the linear transmittance of the sample and γ is the effective three-photon absorption coefficient. γ is directly proportional to the product of σ_2 and an effective excited-state absorption cross section, which is a linear combination of the S_1-S_n and T_1-T_n cross sections. The theory in Figure 6 is determined using no adjustable parameters.

Discussion

As stated in the introduction of this paper, there is interest in systematically comparing the one- and two-photon photophysical properties within a series of chromophores to identify structure property relationships to gain insight into molecular design and engineering of better nonlinear optical materials. The involvement of the singlet and triplet excited-state in the nanosecond nonlinear absorption is important as previously reported[11] so we want to focus our efforts on understanding these properties. To this end, it is important to show that the kinetics and spectral properties obtained via one-photon excitation are needed to understand the differences of nonlinear absorption in the femtosecond and nanosecond domains.

One-Photon Spectral Properties. Addition of branches to the AF240 and AF270 molecules results in only a slight bathochromic (red) shift in all of the spectral data obtained indicating that the degree of conjugation is limited. In the ground-state spectral data and the triplet excited-state data a trend is observed that the molar absorption coefficient becomes larger with increased branches to the material. This is consistent with increased chromophore density or an additive effect from the extra chromophores. In fact, with each addition of an arm the molar absorption coefficient is nearly doubled or tripled that of the dipolar species. It is interesting to note that the S_1-S_n data does not follow the same trend. There is a slight red shift in the data from 550 to 650 nm for AF270 (595 nm), AF295 (595 nm), and AF350 (615 nm), but in this case the dipolar material has the largest molar absorption coefficient followed by AF350 with AF295 the smallest. In the AF240 series, we observe a blue shift in the S_1-S_n absorption maximum from AF240 (623 nm) to AF287 nm (603 nm). The AF380 then red-shifts back slightly to 617 nm. Comparing the singlet excited-state spectra of the AF240 series and the AF270 series reveals that their spectral characteristics are also different. The AF240 series only has one major peak while the AF270 series has two. It is surprising that addition of one phenyl group to the AF270 results in such different characteristics in the singlet excited-state but has only a small effect on the S_0-S_1 and T_1-T_n data.

Looking at the spectral details of these two series of closely related materials reveals that increasing the number of arms results in enhanced absorption intensity in both the ground-state and triplet excited-state spectra. The effect of red-shifting

is only minimal with this addition. Comparing the two series with the AF270 having an additional phenyl ring, it would be expected that the AF270 series would be more conjugated and therefore more red-shifted, but looking at the figures and the data in Table 1 this is not always the case. The fact that the ground-state absorbance of AF240 is red-shifted relative to AF270 reveals that the charge transfer state (S_0-S_1) for AF240 is more stabilized than for AF270 in THF. Perhaps the addition of the phenyl group results in a weaker charge transfer from the nitrogen to the benzothiazole because of (a) increased distance from the donor and acceptor and (b) some deviation of coplanarity in the connection between the phenyl and fluorene moieties in the ground state, or a mixture of both factors a and b.

Kinetic Pathways. Table 2 summarizes all of the kinetic decays observed for each material under various conditions. Upon excitation the excited material quickly reorients itself with the solvent to form a solvent stabilized ICT state that is evident by both the fluorescence Stokes shift and the new species evolved in the femtosecond transient absorption data shown in Figure 3.[18,19] The octupolar materials take the longest for the solvent to reorganize (~2.7 ps), which is because of steric hindrance of the bulkier chromophore. The second lifetime is dual decay from both the S_1 state (localized excited state, LE) and the ICT state to form either the triplet excited-state or to reform the ground state by giving off light through fluorescence or heat through internal conversion. We have determined in this study that the ICT state is formed but not the percentage in the ICT versus the LE state. A detailed study with various solvents would verify the exact percentages.[22] Upon formation of the triplet excited-state, we monitored the decay in both air saturated and deoxygenated conditions. Under air-saturated conditions, the lifetimes are in the nanosecond range, which is typical of most oxygen quenched triplet excited states. The observed trend is that the larger molecules decay faster in the presence of air. Under deoxygenated conditions two lifetimes were found. Overlaying the spectra at different times indicates the formation of a new species. We believe this new species to also be a solvent stabilized ICT state formed from the triplet excited-state based on our previous study of AF455.[2n]

Two-Photon Assisted Excited State Absorption. For many two photon absorbing materials, there is invariably a considerable discrepancy in the two photon absorption cross-sections obtained by differing pulse widths. A dramatic enhancement in the nanosecond regime has been observed repeatedly in many materials and has been termed the effective two-photon cross-section. This enhanced loss in the nanosecond nonlinear data was attributed to excited-state absorption.[23,24] Recently we were able to experimentally confirm that the enhancement in the nanosecond nonlinear absorption of AF240 and AF350 is strongly due to excited-state absorption from both the singlet and triplet excited states.[11] We assume that for other structurally related materials in the AFX family the same would be true.

For the AF240 and AF270 series a comparison is made to predict which material will have large nanosecond nonlinear absorption. This is based on a two-photon-assisted excited-state absorption model where two photons promote the electron to the singlet manifold and then a third photon is absorbed to either promote to higher S_n levels or following intersystem crossing to higher T_n levels. Expansion of eq 2 shows that there are several parameters that are critical in nonlinear absorption of a material and these are shown in eq 7 as the attenuation of the intensity I as light propagates through a sample.[11] Equation 7 incorporates the loss in transmittance due to absorption from the S_1-S_n and T_1-T_n upper excited states:

$$\frac{\partial I}{\partial z} = -\sigma_2 N_{S0} I^2 - \sigma_S N_{S1} I - \sigma_T N_{T1} I \qquad (7)$$

In this equation N_{S0}, N_{S1}, and N_{T1} are the number densities of molecules and σ_2, σ_S, and σ_T are the cross-sections in the S_0, S_1, and T_1 states, respectively. The triplet quantum yield (Φ_T) is also another important parameter because it determines the number density of molecules in the triplet excited state (N_{T1}) so it also must be considered. The critical data has been compiled in Table 3 for comparison. The "Sum" column in the table shows the triplet quantum yield multiplied by the triplet excited-state cross-section because the concentration of triplet excited-state is limited by this value.

By qualitatively comparing the data in Table 3 based on eq 7, it is evident that the contribution from the S_1-S_n state at 800 nm is largest from the octupolar AF350. However, this is not the case for the T_1-T_n. The material with the largest triplet contribution is the octupolar AF380 followed by AF287 and AF295. Based on the femtosecond (fs) TPA cross sections given in Table 3 the octupolar materials have the largest cross section values at 800 nm. Therefore, simply based on a comparison of these values we predict that AF287, AF350, and AF380 will have the largest nonlinear absorption in the nanosecond time regime followed closely by AF295. Traditionally in the literature, the data shown in Figure 6 is fit using eq 1 with $z = 0$ and yields a nanosecond "effective" two-photon cross-section that is significantly larger than the femtosecond value given in column 1 of Table 3. For comparison to literature values we also fit this data to eq 1 with $z = 0$, when the sample is at the focus, and allowed the TPA cross-section to float as a variable parameter. These results are given in the last column of Table 3. The effective TPA cross-sections reveal that AF287, AF350, and AF380 do have the largest nonlinear absorption as we predicted.

In addition to the qualitative comparison we also performed a theoretical fit using eq 6 based on an analytical model that incorporates the parameters given in Table 3 for an effective three-photon absorption.[11] We have thus modeled the system as a two-photon resonant, three-photon absorption medium, and in each calculation there were no free adjustable parameters. The obtained theory is shown in Figure 6 along with the raw experimental data. While the overlap of the experimental and theoretical data is not consistent for every material, these calculations show the large contribution of the excited-state to the overall nonlinear absorption. We believe that the discrepancies in the theoretical data and the actual data are due to a poor determination of the S_1-S_n cross-section at 800 nm. The fundamental laser wavelength in the femtosecond transient absorption is 800 nm so a filter is used to remove most of this light. Therefore, the signal in this region is weak and noisy and more difficult to measure accurately. We are just beginning to understand the various processes involved in nonlinear absorption and hope in the future to improve on the theoretical model. It is true for these materials that the largest nonlinearities arise from AF287 and the octupolar materials as predicted by the linear properties. This shows that measuring the S_1-S_n and T_1-T_n properties of a material is a good linear tool that provides much information about the nanosecond nonlinear absorption of a material.

Conclusions

Structure property relationships of two photon absorbing materials are the key to understanding their nonlinear absorption

properties. In the AF240 and AF270 series we have shown that the effect of adding arms to the central nitrogen atom of the diphenyl amine core results in the octupolar materials having the largest ground-state and triplet excited-state absorption of the series and consequently higher nonlinear absorption, both in the femtosecond and nanosecond regimes. While intersystem crossing is small in all the materials it plays an important role in the overall nonlinear absorbance along with the S_1-S_n absorption. The addition of the phenyl group to the AF270 series results in less formation of the ICT state relative to the AF240 series. The collective union of these properties results in a good starting point for prediction of a material's nonlinear response as evidenced by the theoretical model for these materials.

Acknowledgment. We are thankful for the support of this work by AFRL/ML Contracts FA8650-04-C-5410 for D.G.M. and R.L.S., F33615-94-C-5804 for R.K., F33516-03-D-5421 for J.E.R. and J.E.S. and the Air Force Office of Scientific Research (AFOSR). We thank Evgeny Danilov and Prof. Michael Rodgers for use of the femtosecond transient absorption experiment at the Ohio Laboratory for Kinetic Spectrometry located at Bowling Green State University.

Supporting Information Available: Figures of excitation spectra, emission in various solvents of AF240 and raw z-scan data. This information is available free of charge via the Internet at http:// pubs.acs.org.

References and Notes

(1) (a) Zhao, M.; Samoc, M.; Prasad, P. N.; Reinhardt, B. A.; Unroe, M. R.; Prazak, M.; Evers, R. C.; Kane, J. J.; Jariwala, C.; Sinsky, M. *Chem. Mater*. **1990**, *2*, 670. (b) Pan, H.; Gao, X.; Zhang, Y.; Prasad, P. N.; Reinhardt, B.; Kannan, R. *Chem. Mater*. **1995**, *7*, 816. (c) He, G. S.; Gvishi, R.; Prasad, P. N.; Reinhardt, B. A. *Opt. Commun.* **1995**, *117*, 133. (d) He, G. S.; Xu, G. C.; Prasad, P. N.; Reinhardt, B. A.; Bhatt, J. C.; Dillard, A. G. *Opt. Lett.* **1995**, *20*, 435. (e) He, G. S.; Bhawalkar, J. D.; Prasad, P. N.; Reinhardt, B. A. *Opt. Lett.* **1995**, *20*, 1524. (f) Larson, E. J.; Friesen, L. A.; Johnson, C. K. *Chem. Phys. Lett.* **1997**, *265*, 161. (g) Albota, M.; Beljonne, D.; Bredas, J. L.; Ehrlich, J. E.; Fu, J. Y.; Heikal, A. A.; Hess, S. E.; Kogej, T.; Levin, M. D.; Marder, S. R.; McCord-Maughon, D.; Perry, J. W.; Rockel, H.; Rumi, M.; Subramaniam, G.; Webb, W. W.; Wu, X. L.; Xu, C. *Science* **1998**, *281*, 1653. (h) Chung, S. J.; Kim, K. S.; Lin, T. C.; He, G. S.; Swiatkiewicz, J.; Prasad, P. N. *J. Phys. Chem. B* **1999**, *103*, 10741−10745. (i) Oberle, J.; Bramerie, L.; Jonusauskas, G.; Rulliere, C. *Opt. Commun.* **1999**, *169*, 325. (j) Kotler, Z.; Segal, J.; Sigalov, M.; Ben-Asuly, A.; Khodorkovsky, V. *Synth. Met.* **2000**, *115*, 269. (k) Kim, O. K.; Lee, K. W.; Woo, H. Y.; Kim, K. S.; He, G. S.; Swiatkiewicz, J.; Prasad, P. N. *Chem. Mater*. **2000**, *12*, 284. (l) Adronov, A.; Frechet, J. M. J.; He, G. S.; Kim. K. S.; Chung, S. J.; Swiatkiewicz, J.; Prasad, P. N. *Chem. Mater*. **2000**, *12*, 2838. (m) Rumi, M.; Ehrlich, J. E.; Heikal, A. A.; Perry, J. W.; Barlow, S.; Hu, Z.; McCord-Maughon, D.; Parker, T. C.; Rockel, H; Thayumanavan, S.; Marder, S. R.; Beljonne, D.; Bredas, J. L. *J. Am. Chem. Soc*. **2000**, *122*, 9500. (n) Belfield, K. D.; Bondar, M. V.; Przhonska, O. V.; Schafer, K. J.; Mourad, W. *J. Lumin.* **2002**, *97*, 141. (o) Patra, A.; Pan, M.; Friend, C. S.; Lin, T. C.; Cartwright, A. N. Prasad, P. N. *Burzynski, R. Chem. Mater*. **2002**, *14*, 4044−4048. (p) Martineau, C.; Lemercier, G.; Andraud, C. *Opt. Mater.* **2002**, *21*, 555. (q) Meng, F.; Mi, J.; Qian, S.; Chen, K.; Tian, H. *Polymer* **2003**, *44*, 6851. (r) Mongin, O.; Brunel, J.; Porres, L.; Blanchard-Desce, M. *Tet. Lett.* **2003**, *44*, 2813. (s) Mongin, O.; Porres, L.; Katan, C.; Pons, T.; Mertz, J.; Blanchard-Dexce, M. *Tet. Lett.* **2003**, *44*, 8121. (t) Brousmiche, D. W.; Serin, J. M.; Frechet, J. M. J.; He, G. S.; Lin, T. C.; Chung, S. J.; Prasad, P. *J. Am. Chem. Soc.* **2003**, *125*, 1448. (u) Kamada, K.; Ohta, K.; Iwase, Y.; Kondo, K. *Chem. Phys. Lett.* **2003**, *372*, 386. (v) Drobizhev, M.; Karatoki, A.; Dzenis, Y.; Rebane, A.; Suo, Z.; Spangler, C. W. *J. Phys. Chem. B* **2003**, *107*, 7540. (w) Brousmiche, D. W.; Serin, J. M.; Frechet, J. M. J.; He, G. S.; Lin, T. C.; Chung, S. J.; Prasad, P. N.; Kannan, R.; Tan, L. S. *J. Phys. Chem. B* **2004**, *108*, 8592. (x) Zheng, Q.; He, G. S.; Prasad, P. N. *J. Mat. Chem.* **2005**, *15*, 579. (y) Ahn, T. K.; Kim, K. S.; Kim, D. Y.; Noh, S. B.; Aratani, N.; Ikeda, C.; Osuka, A.; Kim, D. *J. Am. Chem. Soc.* **2006**, *128*, 1700. (z) Wecksler, S. R.; Mikhailovsky, A.; Korystov, D.; Ford, P. C. *J. Am. Chem. Soc*. **2006**, *128*, 3831. (aa) Das, S.; Nag, A.; Goswami, D.; Bharadwaj, P. K. *J. Am. Chem. Soc.* **2006**, *128*, 402.

(2) (a) He, G. S.; Yuan, L.; Cheng, N.; Bhawalkar, J. D.; Prasad, P. N.; Brott, L. L.; Clarson, S. J.; Reinhardt, B. A. *J. Opt. Soc. Am. B* **1997**, *14*, 1079. (b) Reinhardt, B. A.; Brott, L. L.; Clarson, S. J.; Dillard, A. G.; Bhatt, J. C.; Kannan, R.; Yuan, L.; He, G. S.; Prasad, P. N. *Chem. Mater*. **1998**, *10*, 1863. (c) Swiatkiewicz, J.; Prasad, P. N.; Reinhardt, B. A. *Optics Commun.* **1998**, *157*, 135. (d) Joshi, M.; Swiatkiewicz, J.; Xu, F.; Prasad, P. N.; Reinhardt, B. A.; Kannan, R. *Opt. Lett.* **1998**, *23*, 1742. (e) Pudavar, H. E.; Joshi, M. P.; Prasad, P. N.; Reinhardt, B. A. *Appl. Phys. Lett*. **1999**, *74*, 1338. (f) Baur, J. W.; Alexander, M. D.; Banach, M.; Denny, L. R. Reinhardt, B. A.; Vaia, R. A. *Chem. Mater*. **1999**, *11*, 2899. (g) He, G. S.; Swiatkiewics, J.; Jiang, Y.; Prasad, P. N.; Reinhardt, B. A.; Tan, L. S.; Kannan, R. *J. Phys. Chem. A* **2000**, *104*, 4805. (h) Sivaraman, R.; Clarson, S. J.; Lee, B. K.; Steckl, A. J.; Reinhardt, B. A. *Appl. Phys. Lett.* **2000**, *77*, 328. (i) Kannan, R.; He, G. S.; Yuan, L.; Xu, F.; Prasad, P. N.; Dombroskie, A. G.; Reinhardt, B. A.; Baur, J. W.; Vaia, R. A.; Tan, L. S. *Chem. Mater*. **2001**, *13*, 1896. (j) He, G. S.; Lin, T. C.; Prasad, P. N.; Kannan, R.; Vaia, R. A.; Tan, L. S. *J. Phys. Chem. B* **2002**, *106*, 11081. (k) Chiang, L. Y.; Padmawar, P. A.; Canteenwala, T.; Tan, L. S.; He, G. S.; Kannan, R.; Vaia, R.; Lin, T. C.; Zheng, Q.; Prasad, P. N. *Chem. Commun.* **2002**, 1854. (l) Kannan, R.; He, G. S.; Lin, T. C.; Prasad, P. N.; Vaia, R. A.; Tan, L. S. *Chem. Mater*. **2004**, *16*, 185. (m) He, G. S.; Lin, T-C. Dai, J.; Prasad, P. N.; Kannan, R.; Dombroskie, A. G.; Vaia, R. A.; Tan, L. S. *J. Chem. Phys.* **2004**, *120*, 5275. (n) Rogers, J. E.; Slagle, J. E.; McLean, D. G.; Sutherland, R. L.; Sankaran, B.; Kannan, R.; Tan, L. S.; Fleitz, P. A. *J. Phys. Chem. A* **2004**, *108*, 5514. (o) Day, P. N.; Nguyen, K. A.; Pachter, R. *J. Phys. Chem. B* **2005**, *109*, 1803. (p) Nguyen, K. A.; Rogers, J. E.; Slagle, J. E.; Day, P. N.; Kannan, R.; Tan, L. S.; Fleitz, P. A.; Pachter, R. *J. Phys. Chem. A* **2006**, *110*, 13172.

(3) (a) Parthenopoulos, D. A.; Rentzepis, P. M. *Science* **1989**, *249*, 843. (b) Dvornikov, A. S.; Rentzepis, P. M. *Opt. Commun.* **1995**, *119*, 341.

(4) (a) Bhawalkar, J. D.; He, G. S.; Prasad, P. N. *Rep. Prog. Phys.* **1996**, *59*, 1041. (b) He, G. S.; Zhao, C. F.; Bhawalkar, J. D.; Prasad, P. N. *Appl. Phys. Lett.* **1995**, *78*, 3703. (c) Zhao, C. F.; He, G. S.; Bhawalkar, J. D.; Park, C. K.; Prasad, P. N. *Chem. Mater*. **1995**, *7*, 1979.

(5) (a) Fleitz, P. A.; Sutherland, R. A.; Strogkendl, F. P.; Larson, F. P.; Dalton, L. R. *SPIE Proc.* **1998**, *3472*, 91. (b) He, G. S.; Bhawalkar, J. D.; Zhao, C. F.; Prasad, P. N. *Appl. Phys. Lett.* **1995**, *67*, 2433. (c) Ehrlich, J. E.; Wu, X. L.; Lee, L. Y.; Hu, Z. Y.; Roeckel, H.; Marder, S. R.; Perry, J. *Opt. Lett*. **1997**, *22*, 1843.

(6) (a) Kawata, S.; Sun, H. B.; Tanaka, T.; Takada, K. *Nature* **2001**, *412*, 697−698. (b) Cumpston, B. H.; Ananthavel, S. P.; Barlow, S.; Dyer, D. L.; Ehrlich, J. E.; Erskine, L. L.; Heikal, A. A.; Kuebler, S. M.; Le, I. Y. S.; McCord-Maughon, D.; Qin, J.; Rockel, H.; Rumi, M.; Wu, X. L.; Marder, S. R.; Perry, J. W. *Nature* **1999**, *398*, 51.

(7) Denk, W.; Strickler, J. H.; Webb, W. W. *Science* **1990**, *248*, 73.

(8) Bhawalkar, J. D.; Kumar, N. D.; Zhao, C. F.; Prasad, P. N. *J. Clin. Laser Med. Surg.* **1997**, *15*, 201.

(9) (a)Belfield, K. D.; Hagan, D. J.; Van, Stryland, E. W.; Schafer, K. J.; Negres, R. A. *Org. Lett.* **1999**, *1*, 1575. (b) Anemian, R.; Andraud, C.; Nunzi, J.-M.; Morel, Y.; Baldeck, P. L. *SPIE Proc.* **2000**, *4106*, 329. (c) Lee, K.-S.; Yang, H.-K.; Lee, J.-H.; Kim, O.-K.; Woo, H. Y.; Choi, H.; Cha, M. Blanchard-Desce, M. *H. SPIE Proc*. **2003**, *4991*, 175. (d) Lin, T.-C.; He, G. S.; Zheng, Q.; Prasad, P. N. *J. Mat. Chem.* **2006**, *16*, 2490. (e) Schroeder, R.; Ullrich, B. *Opt. Lett.* **2002**, *27*, 1285. (f) Ma, W.; Wu, Y.; Han, J.; Gu, D.; Gan, F. *Chem. Phys. Lett.* **2005**, *403*, 405.

(10) Chung, S.-J.; Kim, K-S.; Lin, T.-C.; He, G. S.; Swiatkiewicz, J.; Prasad, P. N. *J. Phys. Chem. B* **1999**, *103*, 10741.

(11) Sutherland, R. L.; Brant, M. C.; Heinrichs, J.; Rogers, J. E.; Slagle, J. E.; McLean, D. G.; Fleitz, P. A. *J. Opt. Soc. Am. B* **2005**, *22*, 1939.

(12) Sutherland, R. L.; McLean, D. G.; Brant, M. C.; Rogers, J. E.; Fleitz, P. A.; Urbas, A. M. *SPIE Proc.* **2006**, *6330*, 633006.

(13) Rogers, J. E.; Cooper, T. M.; Fleitz, P. A.; Glass, D. J.; McLean, D. G. *J. Phys. Chem. A* **2002**, *106*, 10108−10115.

(14) Demas, J. N.; Crosby, G. A. *J. Phys. Chem.* **1971**, *75*, 991.

(15) Ebbesen, T. W.; Tanigaki, K.; Kuroshima, S. *Chem. Phys. Lett.* **1991**, *181*, 501.

(16) Sheik-Bahae, M.; Said, A. A.; Wei, T.-H.; Hagan, D. J.; Van Stryland, E. W. *IEEE J. Quant. Elect.* **1990**, *26*, 760−770.

(17) Zyss, J. *J. Chem. Phys.* **1993**, *98*, 6583.

(18) Grabowski, Z. R.; Rotkiewicz, K.; Rettig, W. *Chem. Rev.* **2003**, *103*, 3899.

(19) Valeur, B. *Molecular Fluorescence: Principles and Applications*; Wiley-VCH: New York, 2002.

(20) Barbara, P. F.; Jarzeba, W. *Advances in Photochemistry*; John Wiley & Sons, Inc.: New York, 1990; Vol. 15.

(21) Sutherland, R. L. *Handbook of Nonlinear Optics*; Marcel-Dekker, Inc.: New York, 2003.

(22) Schutz, M.; Schmidt, R. *J. Phys. Chem.* **1996**, *100*, 2012.

(23) Kleinschmidt, J.; Rentsch, S.; Tottleben, W.; Wilhelmi, B. *Chem. Phys. Lett.* **1974**, *24*, 133.

(24) Ehrlich, J. E.; Wu, X-L.; Lee, I-Y. X.; Hu, Z-Y.; Rockel, H.; Marder, S. R.; Perry, J. W. *Opt. Lett.* **1997**, *22*, 1843.